

ORBIT STUDIES FOR ION INFLECTORS USED IN CYCLOTRONS*

F. Marti
NSCL, Michigan State University, E. Lansing, Michigan, USA

Summary

Our laboratory has recently commissioned an axial injection line to transport an ECR beam into the K500 superconducting cyclotron, and is in the process of designing a similar line for the K800 cyclotron. Extensive calculations were performed during these studies to evaluate the characteristics of different kinds of ion inflectors at high magnetic fields (3-5 T). Analytic, ray-tracing and transfer matrix techniques were utilized. We compare in this paper the results from the different methods.

Introduction.

Since March 1986, the K500 superconducting cyclotron has been working with an external ECR source¹. The nearly completed K800 cyclotron will also be fitted with an external source. In both cases the beam is injected along the axis of the machine and deflected into the median plane. Most cyclotrons use one of three devices to inject axial beams: electrostatic mirrors², spiral inflectors³ or hyperboloid inflectors⁴. We had selected the electrostatic mirror during our preliminary studies⁵ but the high electric field needed to bend the ions made it undesirable in our case ($V_{inj} = 20$ kV, $Q/u=0.5$, $\rho_m = 8$ mm, $B_0 = 3.62$ T). The spiral inflector developed by Belmont³ at Grenoble requires a lower electric field and although more difficult to machine than the mirror it satisfies our requirement of small size needed to fit inside the first orbit in the central region. One more advantage over the mirror is the absence of grids that decrease the transparency of the device.

The optical properties of ion inflectors are traditionally studied using the linear transfer matrix technique. It is much simpler and faster than numeric integration, and does not require the detailed knowledge of the electric field. It is also simple to include in general programs like TRANSPORT⁶. Due to the small size of our inflector, the beam is always very close to the edge of the electrodes and consequently the fringe field effect could be potentially important during the entire motion inside the inflector. With this possibility in mind we wrote a computer code to integrate the equations of motion in the electric field of the inflector calculated by the relaxation code RELAX3D⁷. We describe in this paper the results of these calculations and compare them with the linear approximation.

Spiral inflector.

The beam at the entrance of the inflector is expected to be 2 mm in diameter approximately. We have selected¹ an inflector gap of 4 mm. The shape of the inflector³ is determined by the magnetic radius of curvature ρ_m and the parameter K, related to the electric radius of curvature A by :

$$K = A / (2\rho_m) \quad (1)$$

$$E = 2 V_{inj} / A \quad (2)$$

where E is the electric field perpendicular to the orbit inside the inflector and qV_{inj} the injection energy. The smaller the value of K, the smaller the horizontal cross-section of the inflector, but also the vertical height of the inflector decreases. As we want A to be significantly larger than the electrode gap, we chose $K=1.1$ as a compromise value.

A comparison between the calculated central ray and the theoretical central ray can be seen in Fig. 1 (top) where we plot the difference in position for both rays as a function of time. The Δx and Δy are taken in the intrinsic (Frenet) coordinate system of the theoretical central ray, along the normal and binormal respectively. The bottom part of the figure shows the electric field components in the laboratory reference frame. We see that the calculated central ray is typically within 0.1 mm of the theoretical position.

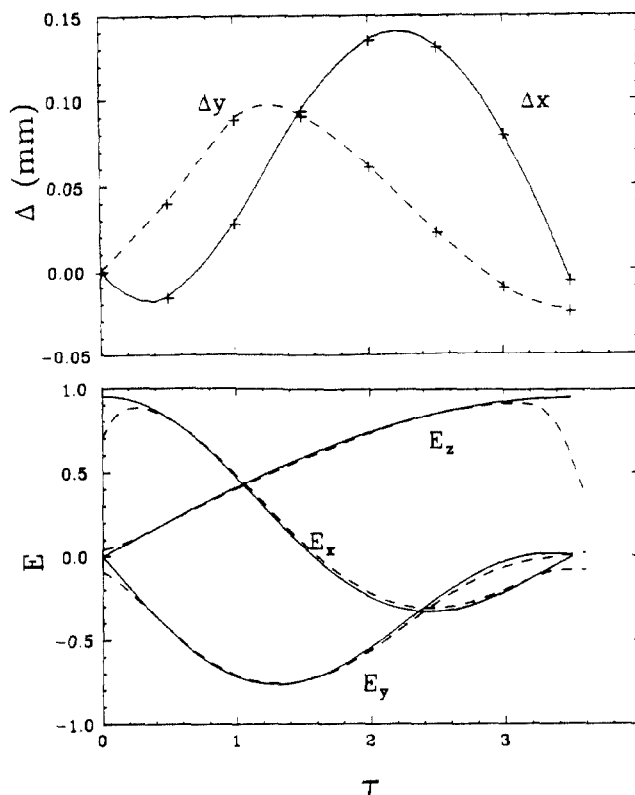


Fig. 1. (Top) Motion of the central ray calculated by numerical integration in the relaxed potential with respect to the theoretical ray. x and y are along the normal and binormal of the theoretical ray ($\tau=wt$). (Bottom) Electric fields (arbitrary units) in the laboratory reference frame for the theoretical ray (solid curve) and the calculated central ray (dashed curve).

* Work supported by NSF under Grant No. PHY-83-12245.

To determine the optical properties of the inflector we tracked particles in the electric field that started displaced from the central ray by $\pm 0.2, 0.4, 0.8,$ and 1.2 mm in the direction perpendicular to the electrodes (X_0) and parallel to them (Y_0). The displacements Δx and Δy , and velocities ΔV_x and ΔV_y with respect to the central ray were calculated in the intrinsic frame. Fig. 2 shows as an example the x components of the displacements divided by the initial displacement. If the system has a linear behavior the normalized displacements should coincide and no difference should be observed between the different

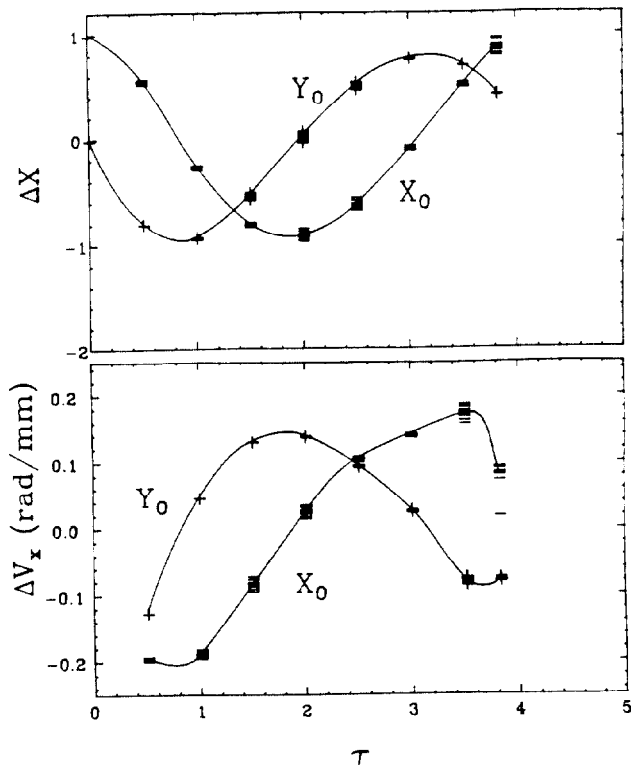


Fig. 2 Transfer matrix elements for the spiral inflector as a function of time τ . X is the coordinate along the normal to the central ray, and eight rays with initial displacements of $\pm 0.2, 0.4, 0.8, 1.2$ mm were calculated and divided by the initial displacement. Two sets were plotted, with displacements perpendicular to the electrodes (X_0) and parallel parallel to them (Y_0).

rays. This is not the case in our calculation and the contributions of the higher order terms are readily observable, especially in the particles that started with an initial displacement perpendicular to the electrodes (X_0). Fig. 3 shows the transit time difference in degrees ($\tau = \omega t, \omega = qB_0/m$) between displaced and central rays.

Similar studies have been performed by Root⁸ for the Triumf inflector with much larger dimensions and less twist ($K=0.4$) than ours. The nonlinear effects were small in their case.

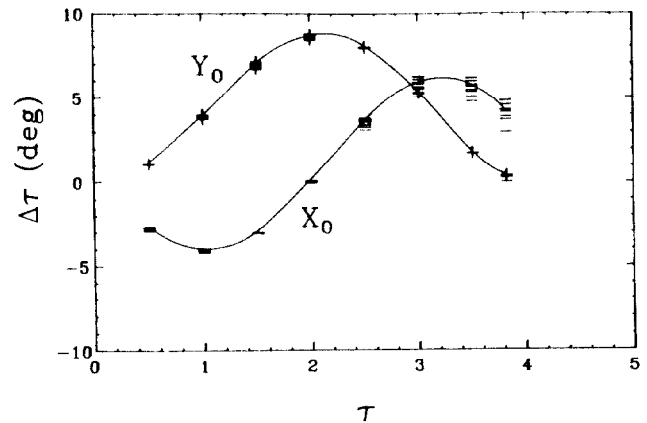


Fig. 3 Normalized time difference between displaced rays and central ray (see Fig. 2).

Hyperboloid inflector.

The hyperboloid inflector developed by Muller⁴ has the advantage over the spiral inflector in that it is easier to machine, because the electrodes are surfaces of revolution. The potential is given by:

$$V = -Kz^2/2 + Kr^2/4 + C \quad (3)$$

where r, θ, z are cylindrical coordinates but not centered in the cyclotron. The machine axis is at $r=r_0$ and $\theta=0$. Aside from edge effects the optics is linear⁹. As in the case of the spiral inflector we calculated the potential in the more realistic model including the RF shield and entrance and exit fringe fields.

The differences between the analytic electric fields and the fields calculated in the relaxed potential are shown in Fig. 4. They are plotted as a percent of the electric field at the entrance of the inflector. The analytic field is taken as zero before the hard edge inflector entrance and after the exit.

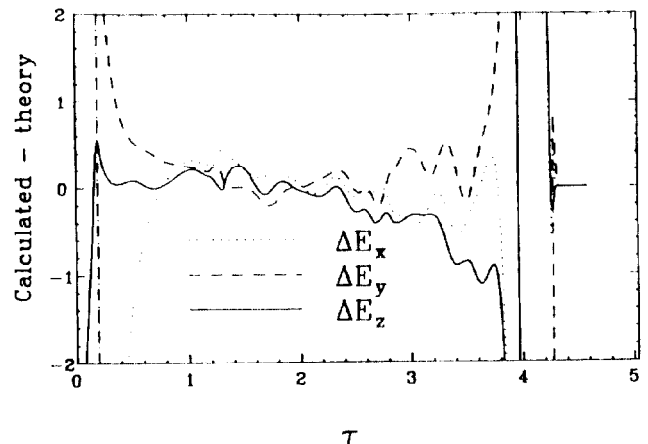


Fig. 4 Difference between the electric field calculated from the relaxed potential along the orbit and the theoretical electric field at the same point in the hyperboloid inflector, as a percent of the field at the inflector entrance.

We see that the difference is well within $\pm 1\%$, except at the edge regions. The details of the edge regions are shown in Fig. 5. We have obtained similar plots for ions that start displaced from the central ray by 1 mm. When the displacement is towards the electrodes the results are noisier, but still within $\pm 1\%$.

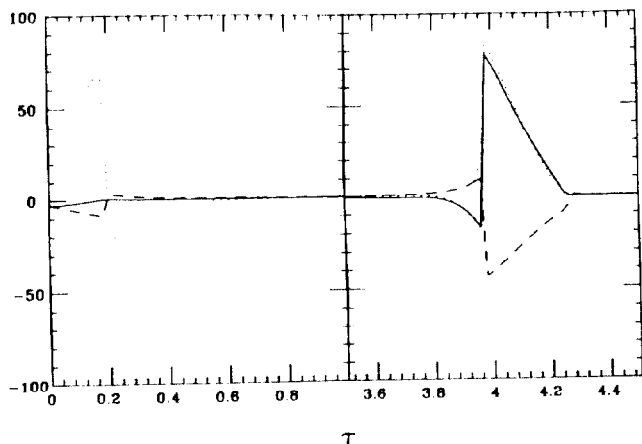


Fig. 5 Similar to Fig. 4 but detailing the entrance and exit regions.

The time evolution of the transfer matrix elements is plotted in Figures 6 and 7. The normalized differences to the central ray were calculated in a way similar to that used for the spiral inflector. The arrows on the right margin indicate the calculated values using a simple edge approximation¹⁰ in the linear transfer matrix. The calculated values agree reasonably well with the numerical integration results.

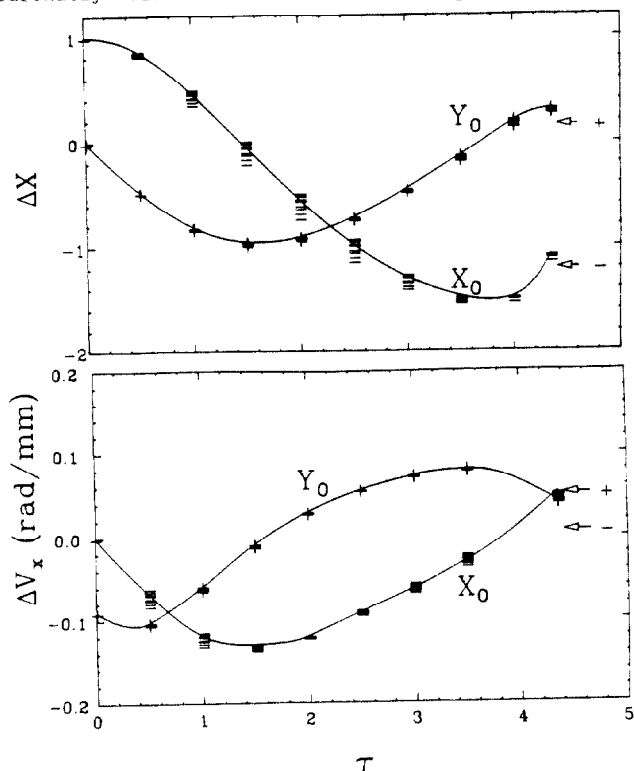


Fig. 6 Similar to Fig. 2, but for the hyperboloid inflector. The arrows on the right margin indicate the expected values calculated with a simple approximation of the edge fields.

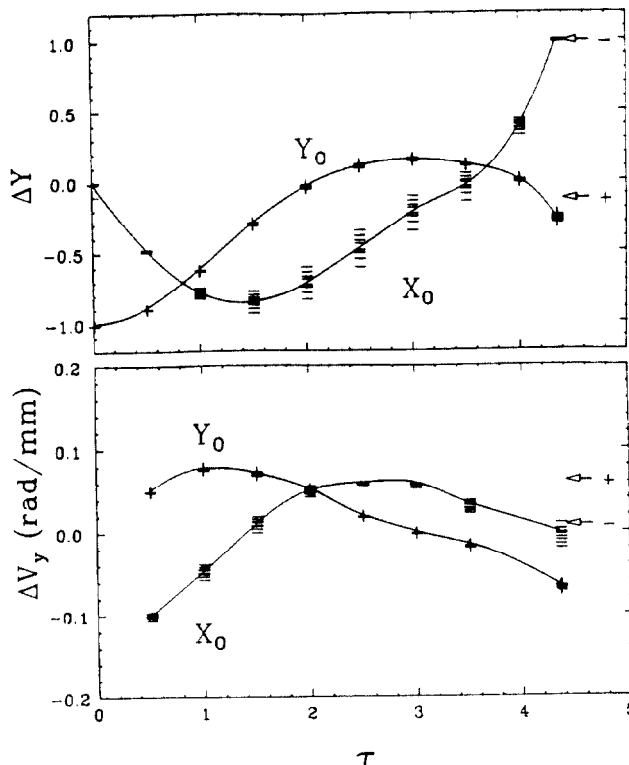


Fig. 7 Similar to Fig. 6. Y is in the direction of the binormal.

Conclusions.

Although the contribution of higher order terms is significant, the multiple advantages of a linear approximation to the motion make it a very desirable tool in the study of ion inflectors. The transfer matrix coefficients determined from analytic approximations seem to be in reasonable agreement with the numerical integration results, but there are exceptions when dealing with small devices and it might be advisable to obtain the coefficients from numerical integration. This is especially true in determining distances to the electrodes when calculating the acceptance of the inflector.

References.

1. F. Marti et al., *IEEE Trans. Nucl. Sci.* NS-32 (1985) 2450.
2. W. B. Powell and B. L. Reece, *Nucl. Instr. and Meth.* 32 (1965) 325.
3. J. L. Belmont and J. L. Pabot, *IEEE Trans. Nucl. Sci.* NS-13 (1966) 191.
4. R. W. Müller, *Nucl. Instr. and Meth.* 54 (1967) 29.
5. G. Bellomo et al., *Nucl. Instr. and Meth.* 206 (1983) 19.
6. K. L. Brown et al., TRANSPORT, CERN 80-04 (1980).
7. H. Houtman and C. J. Kost, Proc. of the Europhysics Conf. on Computing in Acc. design, Springer Verlag (1983).
8. L. W. Root, MSc Thesis, UBC (1972).
9. J.I.M. Botman et al., Proc of the 11th Intl. Conf. on Cyclotrons and their Appl., Tokyo (1986).
10. R. Beck et al., GANIL A.86.02a (1986).